REPORT DOCUMENTATION PAGE

Form Approved
OMB No. 0704-0188

1. AGENCY USE ONLY *(Leave blank)*	2. REPORT DATE	3. REPORT TYPE AND DATES COVERED
	31, July 1997	Technical 6/1/96 - 7/31/96

4. TITLE AND SUBTITLE
Effect of pH, Fluorination, and Number of Layers on the Inhibition of Electrochemical Reactions by Grafted, Hyperbranched Poly(acrylic acid) Films

5. FUNDING NUMBERS
N00014-93-11338
300x084yip
96PR0-1027

6. AUTHOR(S)
M. Zhao, M.L. Bruening, Y. Zhao, D.E. Bergbreiter, R.M. Crooks

7. PERFORMING ORGANIZATION NAME(S) AND ADDRESS(ES)
Department of Chemistry
Texas A&M University
College Station, Texas 77843-3255

8. PERFORMING ORGANIZATION REPORT NUMBER
24

9. SPONSORING / MONITORING AGENCY NAME(S) AND ADDRESS(ES)
Office of Naval Research
800 North Quincy Street
Arlington, Virginia 22217-5000

10. SPONSORING / MONITORING AGENCY REPORT NUMBER

11. SUPPLEMENTARY NOTES
Accepted for publication in *Isr. J. Chem.*

12a. DISTRIBUTION / AVAILABILITY STATEMENT
Reproduction in whole, or in part, is permitted for any purpose of the United States Government. This document has been approved for public release and sale; it's distribution is unlimited.

12b. DISTRIBUTION CODE

13. ABSTRACT *(Maximum 200 words)*

We report the electrode-passivation properties of both fluorinated and unmodified hyperbranched poly(acrylic acid) (PAA) films as a function of pH and the number of PAA layers. Both cyclic voltammetry and ac-impedance spectroscopy show that the extent of blocking increases with the number of layers regardless of the solution pH. However, passivation resulting from unfluorinated PAA films decreases with increasing pH while passivation due to fluorinated films increases with increasing pH. Three-layer fluorinated films can increase the charge transfer resistance of the electrode by up to a factor of 6×10^4. Although Randles' equivalent circuit can be used to model the electrochemistry of electrodes covered with unfluorinated PAA, fluorinated PAA-coated electrodes often require additional circuit elements due to the high resistance of these hydrophobic films.

14. SUBJECT TERMS	15. NUMBER OF PAGES 24
	16. PRICE CODE

17. SECURITY CLASSIFICATION OF REPORT	18. SECURITY CLASSIFICATION OF THIS PAGE	19. SECURITY CLASSIFICATION OF ABSTRACT	20. LIMITATION OF ABSTRACT
Unclassified	Unclassified	Unclassified	

[Submitted for publication as an Article in *Isr. J. Chem.*]

Effect of pH, Fluorination, and Number of Layers on the Inhibition of Electrochemical Reactions by Grafted, Hyperbranched Poly(acrylic acid) Films

Short title: Corrosion Inhibition by Hyperbranched Polymer Films

Key words: Corrosion, Hyperbranched Polymer, Electrochemistry, Self-Assembled Monolayer

Mingqi Zhao, Merlin L. Bruening, Yuefen Zhou,
David E. Bergbreiter*,[1] and Richard M. Crooks*,[2]

Department of Chemistry
Texas A&M University
College Station, TX 77843-3255

[1]phone: 409-845-3437, fax: 409-845-4719
e-mail: bergbreiter@chemvx.tamu.edu
[2]phone: 409-845-5629, fax: 409-845-1399
e-mail: crooks@chemvx.tamu.edu

*Authors to whom correspondence should be addressed

Revised: 10 June, 1997

Abstract

We report the electrode-passivation properties of both fluorinated and unmodified hyperbranched poly(acrylic acid) (PAA) films as a function of pH and the number of PAA layers. Both cyclic voltammetry and ac-impedance spectroscopy show that the extent of blocking increases with the number of layers regardless of the solution pH. However, passivation resulting from unfluorinated PAA films decreases with increasing pH while passivation due to fluorinated films increases with increasing pH. Three-layer fluorinated films can increase the charge transfer resistance of the electrode by up to a factor of 6×10^4. Although Randles' equivalent circuit can be used to model the electrochemistry of electrodes covered with unfluorinated PAA, fluorinated PAA-coated electrodes often require additional circuit elements due to the high resistance of these hydrophobic films.

Introduction

We recently reported initial results demonstrating that surface-grafted, highly fluorinated, hyperbranched poly(acrylic acid) (PAA) films effectively passivate electrode surfaces in basic aqueous solutions.[1] Here we show that PAA films are more passivating at low pH than at high pH while fluorinated PAA films are more passivating under basic conditions. Regardless of pH, however, electrode passivation increases with the number of layers in the film. To model the electrochemistry of the electrode-film interface we employ Randles' and modified Randles' equivalent circuits.[2-4] Modified Randles' equivalent circuits are necessary to account for high resistances in hydrophobic films.

Because corrosion is a very important industrial problem, there are many strategies for corrosion passivation including the deposition of thin, passivating coatings.[5,6] Thin films are deposited by techniques such as spraying, painting, and spin and dip coating. Molecular self-assembly techniques for depositing passivating films may prove especially useful for coating unusual geometries and for on-line modification where spin and dip coating are impractical. The development of self-assembled monolayers (SAMs) showed that even ultrathin layers of highly organized material can block electrochemical reactions and in certain cases reduce the rate of corrosion.[7-15] We are developing corrosion-resistant coatings composed of hyperbranched polymers covalently linked to SAMs via simple chemical reactions. These films are much more durable than SAMs[8-12,16-21] and their ability to span

substrate defects should make them excellent corrosion passivation materials.

Scheme I represents the synthesis and derivatization of PAA films. To prepare hyperbranched PAA films, we first graft poly(*tert*-butyl acrylate) onto a mercaptoundecanoic acid (MUA) monolayer on Au. Hydrolysis of the *tert*-butyl esters then yields a PAA graft and additional grafting at multiple -COOH sites on each prior graft leads to hyperbranched PAA films.[1,22,23] Derivatization of -COOH groups with $H_2NCH_2(CF_2)_6CF_3$ yields a hydrophobic fluorinated film (PAA/F) which effectively passivates metal surfaces (Scheme I). Approximately 50% of the -COOH groups in the film react with $H_2NCH_2(CF_2)_6CF_3$ in one reaction cycle.[23,24] Reactivation of the residual -COOH groups and reaction with $H_2NCH_2(CF_2)_6CF_3$ results in the derivatization of ≈70% of the -COOH groups (Scheme I).[23,24] Here we employ ac-impedance techniques and cyclic voltammetry in an effort to better understand electrode passivation by PAA and fluorinated PAA films at several pH values.

Scheme I

Experimental Section

Film Preparation. PAA, PAA/F, and films fluorinated via two reaction cycles (PAA/2F) were prepared as described previously.[1,22,23]

Chemicals and solutions. $K_4Fe(CN)_6$ and $K_3Fe(CN)_6$ were used as received from Fisher Scientific. 0.2 M CH_3COOH + 0.0036 M CH_3COONa (pH = 3.0), 0.2 M NH_4OH + 0.036 M NH_4Cl (pH = 10.0) and

0.025 M KH_2PO_4 + 0.025 M Na_2HPO_4 (pH = 6.3) were used as buffer solutions. The supporting electrolyte was 1.0 M KCl, which resulted in a solution resistance of 55 Ω between the working and reference electrodes. Aqueous solutions were prepared with 18 MΩ·cm deionized water (Millipore). Before experiments, all solutions were deoxygenated with N_2. During ac-impedance experiments the solution was purged with N_2 at the rate of about two bubbles per second, and during cyclic voltammetry experiments N_2 was gently blown over the solution. All of the experiments were carried out at 22 ± 2 °C.

Cell and electrodes. A three-electrode cell containing a Ag/AgCl (3 M NaCl) reference electrode and a Pt gauze counter electrode (separated from the working electrode by a porous glass plug) was employed in all experiments. The working electrode was a Ti-primed, Au-coated Si wafer[1] sealed in a Teflon holder so as to expose an electrode area of 0.09 cm^2.

Instrumentation. Electrochemical impedance measurements were performed using an EG&G PARC 273A (EG&G, Princeton, NJ) potentiostat and a Solartron 1255 frequency response analyzer (Solartron, Allentown, PA) controlled by a microcomputer running Z-PLOT software (Scribner Associates, Charlottesville, VA). Impedance measurements were performed using a 5 mV rms sine wave around E^o of $Fe(CN)_6^{3-/4-}$, and readings were taken at five discrete frequencies per decade. The impedance results were analyzed using Z-PLOT and ZSIM/CNLS software (Scribner Associates). The cyclic voltammetry experiments were carried out using a BAS 100A

Electrochemical Analyzer (Bioanalytical Systems, West Lafayette, IN) using $Fe(CN)_6^{3-}$ as the electroactive species.

Results and Discussion

We recently showed that fluorinated, 3-layer PAA films (3-PAA/F) effectively passivate Au electrodes in basic aqueous solutions (pH = 10).[1] 3-PAA/F films are approximately 10 times more effective at blocking electron-transfer reactions than a hexanedecanethiol ($C_{16}SH$) SAM and are also much more stable than SAMs to electrochemical cycling.[1] In this section, we examine the effects of pH and the number of PAA layers on electrode passivation. In addition, we discuss film structures and equivalent circuit models of the electrode-film-solution interfaces.

Electrode passivation and the number of PAA layers. Electrode passivation increases with the number of PAA layers because of increases in both film thickness and branching. New branches in the film can block access to underlying pinholes leading to the electrode surface. Figure 1a shows cyclic voltammetry (0.005 M $Fe(CN)_6^{3-}$, pH 10) of electrodes covered with 1-layer (1-PAA), 2-layer (2-PAA), and 3-layer (3-PAA) PAA films.[25] The results show that current decreases significantly as the number of PAA layers increase. Additionally, the shape of the voltammogram changes from that characteristic of linear diffusion to a macroelectrode (peak-shaped voltammogram) in the case of a 1-PAA film to that characteristic of radial diffusion to an array of microelectrodes[26,27] (steady-state current) upon the addition of

the second and third PAA layers. The same trends occur for fluorinated (Figure 1b) and doubly-fluorinated (Figure 1c) PAA films. Similar behavior obtains in pH 3- and pH 6-buffered solutions although the magnitude of the current varies with pH (*vide infra*).

Figure 1

In addition to cyclic voltammetry, we employed ac-impedance spectroscopy to study these film-coated electrodes. Impedance spectroscopy is a very effective tool for the characterization of polymer film-modified electrodes because the system is only marginally perturbed due to the very low-amplitude, sinusoidal voltages (in this case 5 mV rms) that are used, and because measurements can provide information about electrode capacitances (double-layer and film capacitance), charge-transfer kinetics, and ohmic resistance.[2,28-30] However, the disadvantage of ac-impedance techniques is that the results are sometimes difficult to interpret.[31-35] To facilitate interpretation, we chose to study the simple, one-electron redox reaction involving $Fe(CN)_6^{3-}$ /$Fe(CN)_6^{4-}$ and utilized Randles' or a modified Randles' equivalent circuit to model the experimental results.

Figure 2 shows Nyquist plots (complex-plane impedance plots) for electrodes coated with PAA and fluorinated PAA films. In pH 3-buffered solution, R_{ct} (which is approximately equal to the diameter of the semicircle in the Nyquist plot) of a 3-layer PAA-coated electrode is 500 times that of a 1-layer PAA-coated

electrode. Similarly, R_{ct} of a 3-PAA/F-covered electrode is 10 times that of 1-PAA/F-coated surface. Table 1 contains the values of R_{ct} and film thicknesses for electrodes modified with different PAA films. These data reveal that in both fluorinated and unfluorinated films, R_{ct} increases with the number of layers but does not scale directly with film thickness. This shows that the effects of film structure (i.e., branching) on electrode passivation are not simply due to increases in film thickness.

Figure 2

Table 1

Table 1 also contains estimates of the fraction of the electrode surface which is electrochemically active (1-θ). To estimate the value of (1-θ), we used eq. 1:

$$1-\theta = \frac{R_{ct}^{o}}{R_{ct}} \qquad (1)$$

where R_{ct}^{o} is the charge-transfer resistance of naked Au and R_{ct} is the charge transfer resistance of the modified electrode. Eq 1 assumes that electron transfer at coated electrodes occurs only at regions that are accessible and not covered by the film. Because electron tunneling through the film may occur in some cases, values of 1-θ should be viewed with caution.[36]

Scheme II shows the model of PAA-coated Au electrodes that we used to interpret the ac-impedance results. The MUA SAM contains many pinholes and does not effctively passivate the electrode.

Most of these pinholes are blocked by grafting PAA to the SAM. Although the highly branched PAA film may also contain some channels, most of these terminate directly within the film. The few remaining locations on the Au surface that are accessible to the solution will behave as an assembly of microelectrodes.

Scheme II

Electrode passivation as a function of pH. Using Fourier transform infrared-external reflection spectroscopy (FTIR-ERS), we previously showed that PAA films can be deprotonated in basic aqueous solutions.[24] Even at pH 6, most acid groups are deprotonated. Ionization of the film and the accompanying reduction in hydrogen bonding capacity cause the "dry" film thickness to increase by about 40% as shown by ellipsometry.[24] Such changes in film properties greatly affect electrode passivation.

Figure 3 shows impedance plots for electrodes coated with 3-PAA and 3-PAA/F films in pH 3.0-, 6.3-, and 10.0-buffered solutions. For the 3-PAA film-modified electrodes, R_{ct} decreases significantly with increasing pH. Although the thickness of 3-PAA films increases upon deprotonation of -COOH groups, the films are still more permeable because of increased hydrophilicity and weaker interchain interactions.

Figure 3

Because single-cycle derivatization of 3-PAA films with $H_2NCH_2(CF_2)_6CF_3$ occurs in about 50% yield,[24] PAA/F films still contain a large number of -COOH groups and should also be affected by changes in pH. Surprisingly, R_{ct} for fluorinated films increases with increasing pH (Figure 3). We speculate that this effect may be due to pH-dependent phase segregation of the hydrophobic $H_2NCH_2(CF_2)_6CF_3$ pendant groups[37] or exclusion of negatively charged electroactive species due to electrostatic repulsion by unreacted $-COO^-$ groups in the film. Underivatized PAA films may not show this effect because of a large film expansion that occurs upon deprotonation.[38]

Cyclic voltammetry corroborates the impedance results. As shown in Figure 4, the Faradaic current at PAA-coated electrodes (e.g., 2-PAA and 3-PAA), increases with increasing pH due to the more open structure of ionized films. In constrast, 3-PAA/F-coated electrodes yield decreases in current with increases in pH (Figure 5). On going from a pH 10- to a pH 3-solution, the cyclic voltammetry of 3-PAA-coated electrodes changes from plateau shaped to one that is characteristic of very slow electron-transfer kinetics or possibly tunneling. On the other hand, the plateau currents for the 3-PAA/F- and 3-PAA/2F-covered electrodes increase significantly upon going from a pH 10 to a pH 3 solution (Figure 5). Unexpectedly, the magnitude of the current for 3-PAA/2F-coated electrodes (at a particular pH) is slightly larger than that at 3-PAA/F-coated surfaces in spite of the greater hydrophobicity and fluorine content of PAA/2F films. Although, we

do not yet understand this phenomenon, it may be related to the two effects mentioned at the end of the previous paragraph.

Figure 4

Figure 5

Models for PAA- and fluorinated PAA-coated electrodes. Cyclic voltammetry suggests that some of the hyperbranched polymer film-coated electrodes behave as an array of microelectrodes. For electrodes modified with 3-PAA and 3-PAA/F films, plateau (rather than peak) currents characteristic of a microelectrode array appear in all of the voltammetry discussed here (scan rates from 1-500 mV/sec). In the case of thinner films, such as 2-PAA, the shape of the voltammogram can depend upon the scan rate as shown in Figure 6. In pH 10-buffered solutions, electrodes covered with 2-PAA films show peak currents at low scan rates (≤10 mV/s), while at higher scan rates, only plateau currents occur. This indicates that the pinholes in this film are sufficiently close together that at low scan rates their diffusion layers overlap resulting in linear rather than radial diffusion.[39]

Figure 6

Nyquist plots also point to microelectrode array-like behavior for multilayer film-coated Au surfaces. For 3-PAA and 3-PAA/F films in both acidic and basic solutions, the low-frequency 45° line characteristic of Warburg diffusion does not appear.

(Figure 3) This is likely due to the fact that complex diffusion mechanisms (rather than linear diffusion) occur.

The dominance of the semicircular region of the Nyquist plots for 2- and 3-layer film-coated Au electrodes (Figures 2 and 3) indicates that reactions at the modified electrodes are kinetically controlled over a wide frequency range. Kinetic control demonstrates that diffusion through the film to active areas of the electrode is not rate limiting. This is consistent with the enhanced mass transfer resulting from the radial diffusion mechanism suggested by cyclic voltammetry.

Equivalent circuits. The impedance of a film-coated electrode is often too complex to be described by Randles' equivalent circuit. In the present case, the film on the surface of the electrode adds another capacitance to the circuit as well as an additional resistance as shown in Figure 7a. When the resistance to current flow through the film (R_f) is negligibly small, the total capacitance (C_t) is equal to the sum of the film capacitance (C_f) and the double-layer capacitance (C_{dl}). The circuit of Figure 7a then reduces to Randles' equivalent circuit (Figure 7b).

Figure 7

R_f should be small in the case of hydrophilic PAA films, but much larger for hydrophobic fluorinated films. The Bode plot (phase angle vs. log frequency) for PAA film-covered electrodes (Figure 8b, for example) contains only one peak, while the same

plot for 3-PAA/2F-coated electrodes (Figure 8d) has two peaks. The high frequency peak in the Bode plot suggests an additional time constant due to R_f and C_f.[40] We simulated the Bode and Nyquist plots for PAA- and fluorinated PAA-coated electrodes using equivalent circuits 7a and 7b and the results are shown in Figure 8 and Table 2. We find that the simple Randles' equivalent circuit (Figure 7b) fits all electrodes coated with PAA and some of the thinner fluorinated film-covered electrodes fairly well. However, a modified Randles' equivalent circuit (Figure 7a) is necessary to obtain a reasonable fit to the Bode plot for electrodes covered with thicker, fluorinated films. The R_{ct} values derived from simulations using the modified Randles' equivalent circuit are within 25% of R_{ct} values obtained using Z-PLOT to fit the semicircular portion of the Nyquist plots. Thus, although the fluorinated film-covered electrodes are quite complex, the diameter of the semicircle in the Nyquist plots is still representative of R_{ct}.

Table 2

Figure 8

Film capacitance. Table 3 contains C_t values for film-coated electrodes in several different buffer solutions. The value of C_t reflects a combination of C_f and C_{dl} and can sometimes be described by the eq 2 where C_f^o , C_{dl}^o , and θ are the pinhole-free film capacitance, the double-layer capacitance of naked Au, and the fractional surface coverage of the film, respectively.[36,41,42]

$$C_t = C_{dl} + C_f = C_{dl}^{o}(1-\theta) + C_f^{o}(\theta) \qquad (2)$$

Table 3

Although eq 2 may not apply quantitatively to hyperbranched PAA films because of their complex, layered structure, it should still be qualitatively useful. Generally C_t is dominated by C_{dl}^{o} at low surface coverage and by C_f^{o} at high surface coverage. In pH 3.0-buffered solutions, C_t decreases as the number of layers in the film increases (Table 3). This is due to an increase in θ as well as a decrease in C_f^{o} due to increasing thickness ($C_f^{o} = \varepsilon_f\varepsilon^{o}/d$, where d is the thickness of the film, ε_f is its dielectric constant and ε^{o} is the permittivity of free space). In pH 6.3-buffered solutions, however, the decrease in capacitance with the number of layers does not occur. This reflects the complex structure of these films.

For a particular film, when the pH changes from 3 to 10, there are several factors that affect C_t: extent of ionization, thickness, and surface coverage (θ). Increases in ε due to ionization will increase C_t. Thickness increases upon ionization, on the other hand, should decrease C_t. Changes in θ due to pH variation depend on whether or not the film is fluorinated and so the effect of coverage on C_t will vary with the composition of the film. Therefore, the effect of pH on C_t is complicated and depends on whether extent of ionization, thickness, or surface

coverage dominates film behavior. For 1-, 2-, and 3-layer PAA films, the capacitance increases on going from pH 3.0 to higher pH values likely due to a significant increase in the film dielectric constant upon ionization (Table 3). The relation between pH and C_t for fluorinated films is irregular reflecting the complex chemical and structural aspects of the film.

Conclusions

Fluorinated and non-fluorinated 3-layer hyperbranched PAA films greatly reduce the active area of electrodes and are therefore candidates for corrosion-inhibiting coatings. Changes in solution pH affect the structure of PAA and fluorinated PAA films resulting in changes in the extent of electrode passivation. Unfluorinated PAA films are less blocking in basic conditions because deprotonation of the -COOH groups makes the film more open and hydrophilic. In contrast, 3-layer fluorinated films become more blocking in basic solutions. This may result from pH-dependent phase segregation of hydrophobic, fluorinated pendant groups. Passivation resulting from PAA/2F films is slightly less than that due to PAA/F films. We employed Randles' and modified Randles' equivalent circuits to simulate the ac-impedance results. While PAA film-covered electrodes can be adequately modeled by Randles' equivalent circuit, fluorinated films require an additional film resistance and capacitance due to their extreme hydrophobicity.

Acknowledgments

We are grateful for financial support of this research from the office of Naval Research (R. M. C.), the National Science Foundation (D. E. B.: DMR-9634196) and the State of Texas Higher Education Coordinating Board through the Advanced Technologies Program. M. L. B. acknowledges a NIH postdoctoral fellowship.

References

(1) Zhao, M.; Zhou, Y.; Bruening, M. L.; Bergbreiter, D. E.; Crooks, R. M. *Langmuir* **1997**, *13*, 1388.

(2) Bard, A. J.; Faulkner, L. R. *Electrochemical Methods: Fundamentals and Applications*; John Wiley & Sons, Inc.: New York, 1980, pp 718.

(3) Inzelt, G.; Láng, G. *J. Elecroanal. Chem.* **1994**, *378*, 39.

(4) Rubinstein, I.; Sabatani, E.; Rishpon, J. *J. Electrochem. Soc.* **1987**, *134*, 3078.

(5) *Fundamental Aspects of Corrosion Protection By Surface Modification*; McCafferty, E.; Clayton, C. R., Eds.; The Electrochemical Society: Pennington, NJ, 1984; Vol. 84-3, pp 355.

(6) Fontana, M. G.; Greene, N. D. *Corrosion Engineering;* 2nd ed.; McGraw-Hill: New York, 1978, pp 465.

(7) Nuzzo, R. G.; Allara, D. L. *J. Am. Chem. Soc.* **1983**, *105*, 4481.

(8) Laibinis, P. E.; Whitesides, G. M. *J. Am. Chem. Soc.* **1992**, *114*, 9022.

(9) Porter, M. D.; Bright, T. B.; Allara, D. L.; Chidsey, C. E. D. *J. Am. Chem. Soc.* **1987**, *109*, 3559.

(10) Yamamoto, Y.; Nishihara, H.; Aramake, K. *J. Electrochem. Soc.* **1993**, *140*, 436.

(11) Li, Y.-Q.; Chailapakul, O.; Crooks, R. M. *J. Vac. Sci. Technol. B.* **1995**, *13*, 1300.

(12) Zamborini, F. P.; Crooks, R. M. *Langmuir* **1997**, *13*, 122.

(13) Itoh, M.; Nishihara, H.; Aramaki, K. *J. Electrochem. Soc.* **1994**, *141*, 2018.

(14) Itoh, M.; Nishihara, H.; Aramaki, K. *J. Electrochem. Soc.* **1995**, *142*, 3696.

(15) Itoh, M.; Nishihara, H.; Aramaki, K. *J. Electrochem. Soc.* **1995**, *142*, 1839.

(16) Finklea, H. O.; Snider, D. A.; Fedyk, J. *Langmuir* **1990**, *6*, 371.

(17) Finklea, H. O.; Snider, D. A.; Fedyk, J.; Sabatani, E.; Gafni, Y.; Rubinstein, I. *Langmuir* **1993**, *9*, 3660.

(18) Widrig, C. A.; Chung, C.; Porter, M. D. *J. Electroanal. Chem.* **1991**, *310*, 335-359.

(19) Walczak, M. M.; Popenoe, D. D.; Deinhammer, R. S.; Lamp, B. D.; Chung, C.; Porter, M. D. *Langmuir* **1991**, 7, 2687.

(20) Weisshaar, D. E.; Walczak, M. M.; Porter, M. D. *Langmuir* **1993**, *9*, 323.

(21) Tarlov, M. J.; Newman, J. G. *Langmuir* **1992**, *8*, 1398.

(22) Zhou, Y.; Bruening, M. L.; Bergbreiter, D. E.; Crooks, R. M.; Wells, M. *J. Am. Chem. Soc.* **1996**, *118*, 3773.

(23) Zhou, Y.; Bruening, M. L.; Bergbreiter, D. E.; Crooks, R. M. *Langmuir* **1996**, *12*, 5519.

(24) Bruening, M. L.; Zhou, Y.; Aguilar, G.; Agee, R.; Bergbreiter, D. E.; Crooks, R. M. *Langmuir* **1997**, *13*, 770.

(25) The cyclic voltammograms contain a small anodic current at the starting potential (500 mV vs. Ag/AgCl) due to the oxidation of Au in the presence of a high concentration of Cl^-.

(26) Amatore, C.; Savéant, J. M.; Tessier, D. *J. Electroanal. Chem.* **1983**, *147*, 39.

(27) Menon, V. P.; Martin, C. R. *Anal. Chem.* **1995**, *67*, 1920.

(28) Sluyters-Rehbach, M.; Sluyters, J. H. In *Electroanalytical Chemistry*; A. J. Bard, Ed.; Marcel Dekker: New York, 1970; Vol. 4., p 1.

(29) *Proceedings of the First International Symposium on Electrochemical Impedance Spectroscopy*; Gabrielli, C., Ed.; Electrochim. Acta: 1990; Vol. 35.

(30) *Proceedings of the Second International Symposium on Electrochemical Impedance Spectroscopy*; Macdonald, D. D., Ed.; Electrochim. Acta: 1993; Vol. 38.

(31) Macdonald, J. R. *J. Electroanal. Chem* **1987**, *223*, 25.

(32) Macdonald, J. R. *J. Appl. Phys.* **1987**, *62*, R51.

(33) Macdonald, J. R.; Hurt, R. L. *J. Electroanal. Chem.* **1986**, *200*, 69.

(34) Hurt, R. L.; Macdonald, J. R. *Solid State Ionics* **1986**, *20*, 111.

(35) Orazem, M. E.; Agarwal, P.; Garcia-Rubio, L. H. *J. Electroanal. Chem.* **1994**, *378*, 51.

(36) Sabatani, E.; Cohen-Boulakia, J.; Bruening, M.; Rubinstein, I. *Langmuir* **1993**, *9*, 2974.

(37) Sun, F.; Castner, D. G.; Mao, G.; Wang, W.; McKeown, P.; Grainger, D. W. *J. Am. Chem. Soc.* **1996**, *118*, 1856.

(38) Unpublished results.

(39) Chailapakul, O.; Crooks, R. M. *Langmuir* **1995**, *11*, 1329.

(40) Cahan, B. D.; Chen, C. T. *J. Electrochem. Soc.* **1982**, *129*, 700.

(41) Sabatani, E.; Rubinstein, I. *J. Phys. Chem.* **1987**, *91*, 6663.

(42) Sabatani, E.; Rubinstein, I.; Maoz, R.; Sagiv, J. *J. Electroanal. Chem.* **1987**, *219*, 365.

Table 1. Total film thickness[a] (d), charge-transfer resistance[a] (R_{ct}) and fractional active electrode area[a] (1-θ) of PAA and fluorinated PAA-coated electrodes.

Electrode	d, Å	pH = 3.0		pH = 6.3		pH = 10.0	
		R_{ct}	1-θ	R_{ct}	1-θ	R_{ct}	1-θ
bare gold[b]	-	1.4	1	1.3	1	1.1	1
Au/MUA[b]	13	79	0.017	18	0.070	3.4	0.32
Au/1-PAA[b]	30	67	0.020	15	0.083	16	0.071
Au/1-PAA/F[b]	50	570	0.0024	580	0.0022	650	0.0017
Au/1-PAA/2F[b]	60	130	0.010	350	0.0036	240	0.0052
Au/2-PAA[b]	130	2.3k	0.00058	720	0.0017	400	0.0027
Au/2-PAA/F[c]	240	3.9k	0.00035	9.7k	0.00013	22k	0.00005
Au/2-PAA/2F[c]	200	1.8k	0.00076	3.3k	0.00038	2.2k	0.00051
Au/3-PAA[b]	370	34k	0.00004	14k	0.00009	1.8k	0.00061
Au/3-PAA/F[c]	800	6.3k	0.00021	12k	0.00010	65k	0.00002
Au/3-PAA/2F[c]	960	4.3k	0.00032	5.4k	0.00023	21k	0.00005

[a]These are values for a specific sample. Total thickness and R_{ct} values can vary by up to 50% from sample to sample, but the relative trends in R_{ct} shown in the table are consistent.

[b]The charge-transfer resistance (R_{ct}) of these electrodes was obtained by analyzing log|Z| vs. log(ω) plots.

[c]The charge-transfer resistance (R_{ct}) of these electrodes was obtained using Z-PLOT software to fit the semicircle of Nyquist plots at intermediate frequencies.

Table 2. Capacitance and resistance values of modified Au electrodes in pH 10 solution. Data were obtained from impedance plots (exp) or from simulation (sim) of impedance data using Randles' and modified Randles' equivalent circuits (see Figure 7).

Electrode	$R_{f,sim}$ Ω-cm^2	$C_{f,sim}$ μF/cm^2	$R_{ct,exp}$[a] Ω-cm^2	$R_{ct,sim}$ Ω-cm^2	$C_{t,exp}$[a] μF/cm^2	$C_{t,sim}$ μF/cm^2
Au/1-PAA[b,c]	-	-	16	14	6.5	7.0
Au/2-PAA[b,c]	-	-	400	330	6.5	6.0
Au/3-PAA[b,d]	-	-	1.8k	1.8k	5.7	6.2
Au/3-PAA/F[d,e]	6.0k	3.5	65k	49k	5.3	2.9
Au/3-PAA/2F[d,e]	69	1.2	20k	21k	7.4	5.8

[a]Experimental data were obtained using the methods denoted in Table 1 and Table 3.

[b]Simulated with Randles' equivalent circuit.

[c]The Warburg diffusion element (semi-infinite linear diffusion) was used in these equivalent circuit simulations.

[d]The very general constant phase diffusion element was used in these equivalent circuit simulations. This element is useful for high surface-coverage films.

[e]Simulated with a modified Randles' equivalent circuit (Figure 7a).

Table 3. Total capacitance (C_t) of naked, MUA-, PAA-, and fluorinated PAA-coated Au electrodes.

Electrode	pH = 3.0	pH = 6.3	pH = 10.0
	C_t[a] ($\mu F/cm^2$)	C_t[a] ($\mu F/cm^2$)	C_t[a] ($\mu F/cm^2$)
naked Au	34	31	23
Au/MUA	2.5	3.2	4.1
Au/1-PAA	5.7	6.5	6.5
Au/1-PAA/F	9.4	7.8	6.5
Au/1-PAA/2F	13	7.5	8.7
Au/2-PAA	4.0	5.3	6.5
Au/2-PAA/F	5.7	7.1	7.2
Au/2-PAA/2F	1.1	0.55	4.8
Au/3-PAA	3.6	6.3	5.7
Au/3-PAA/F	0.41	3.9	5.3
Au/3-PAA/2F	0.53	1.7	7.4

[a]Data were obtained by analyzing $\log|Z|$ versus $\log(\omega)$ plots.

Figure Captions

Figure 1. Cyclic voltammetry of Au electrodes coated with 1-3 layers of PAA or fluorinated PAA films (5 mM $Fe(CN)_6^{3-}$, pH = 10, 50 mV/s).

Figure 2. Complex-plane impedance plots for Au electrodes coated with 1-3 layers of PAA or fluorinated PAA. Data were obtained in a pH 3.0-buffered aqueous solution containing 5 mM $Fe(CN)_6^{3-}$ and 5 mM $Fe(CN)_6^{4-}$. Frequencies (Hz) are given for some of the data points. The data are from a representative sample. R_{ct} values (and film thickness) can vary by up to 50% from sample to sample, but the relative trends in R_{ct} shown in the figure are consistent.

Figure 3. Complex-plane impedance plots for Au electrodes coated with 3-PAA or fluorinated 3-PAA films. Data were obtained in pH 3.0-, pH 6.3- or pH 10.0-buffered aqueous solution containing 5 mM $Fe(CN)_6^{3-}$ and 5 mM $Fe(CN)_6^{4-}$. Frequencies (Hz) are given for some of the data points.

Figure 4. Cyclic voltammetry of 2-PAA- and 3-PAA-coated electrodes in pH 3.0-, pH 6.3-, and pH 10.0-buffered aqueous solutions containing 5 mM $Fe(CN)_6^{3-}$. Scan rate: 50 mV/s.

Figure 5. Cyclic voltammetry of 3-PAA- (triangles), fluorinated 3-PAA- (X's), and doubly fluorinated 3-PAA- (circles) coated

electrodes in pH 3.0- and pH 10.0-buffered aqueous solutions containing 5 mM $Fe(CN)_6^{3-}$. Scan rate: 50 mV/s.

Figure 6. Cyclic voltammetry of 2-PAA-coated electrodes in pH 10.0-buffered aqueous solutions containing 5 mM $Fe(CN)_6^{3-}$ obtained at scan rates ranging from 10 to 500 mV/s.

Figure 7. Modified (a) and unmodified (b) Randles' equivalent circuits used to simulate experimental results.

Figure 8. Experimental (open circles) and simulated (filled circles) Nyquist and Bode plots for 2-PAA and 3-PAA/2F-coated electrodes. The solid circles represent the simulation with Randles' equivalent circuit (2-PAA) or a modified Randles' equivalent circuit (3-PAA/2F).

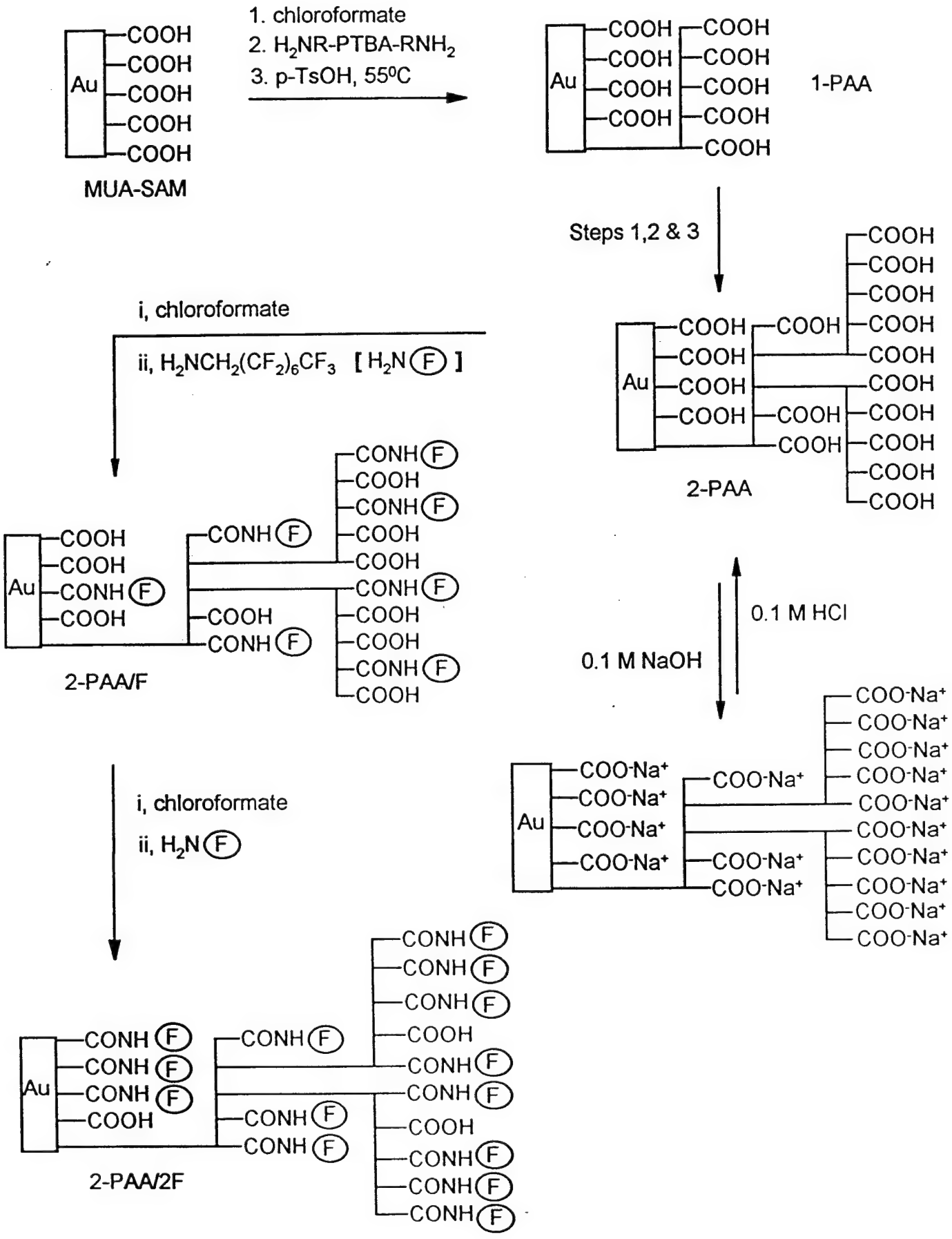
1. chloroformate
2. H_2NR-PTBA-RNH_2
3. p-TsOH, 55°C
Au
COOH
MUA-SAM
1-PAA
Steps 1,2 & 3
2-PAA
i, chloroformate
ii, $H_2NCH_2(CF_2)_6CF_3$ [H_2N(F)]
CONH(F)
2-PAA/F
0.1 M HCl
0.1 M NaOH
COO^-Na^+
i, chloroformate
ii, H_2N(F)
2-PAA/2F

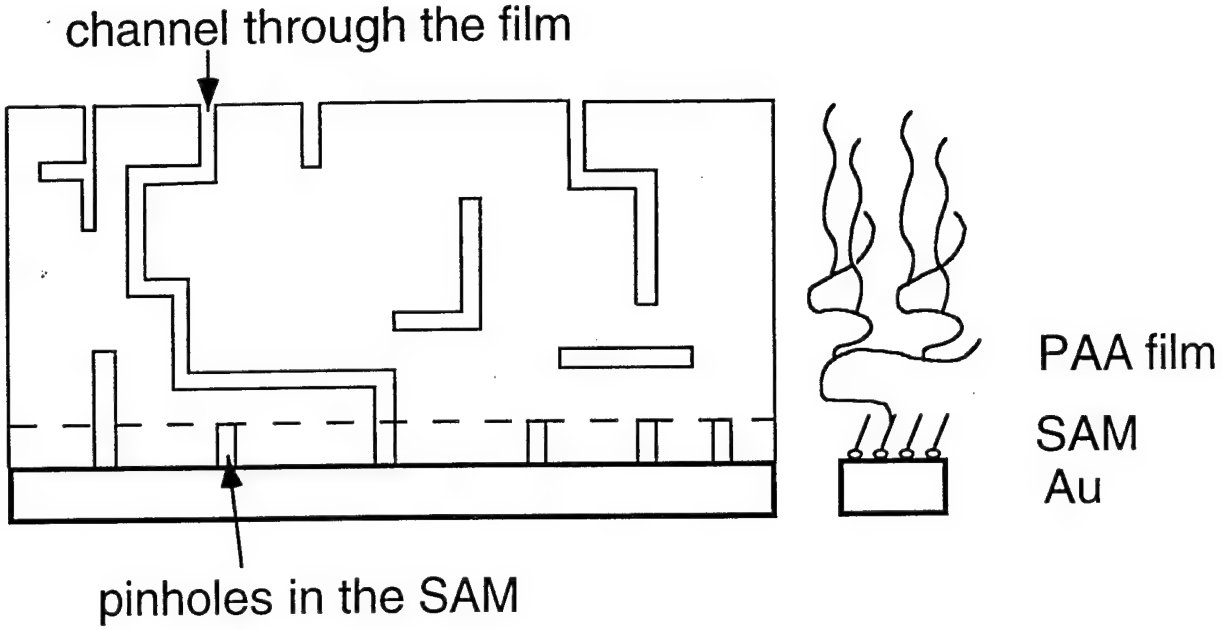

Scheme II / Zhao et al.

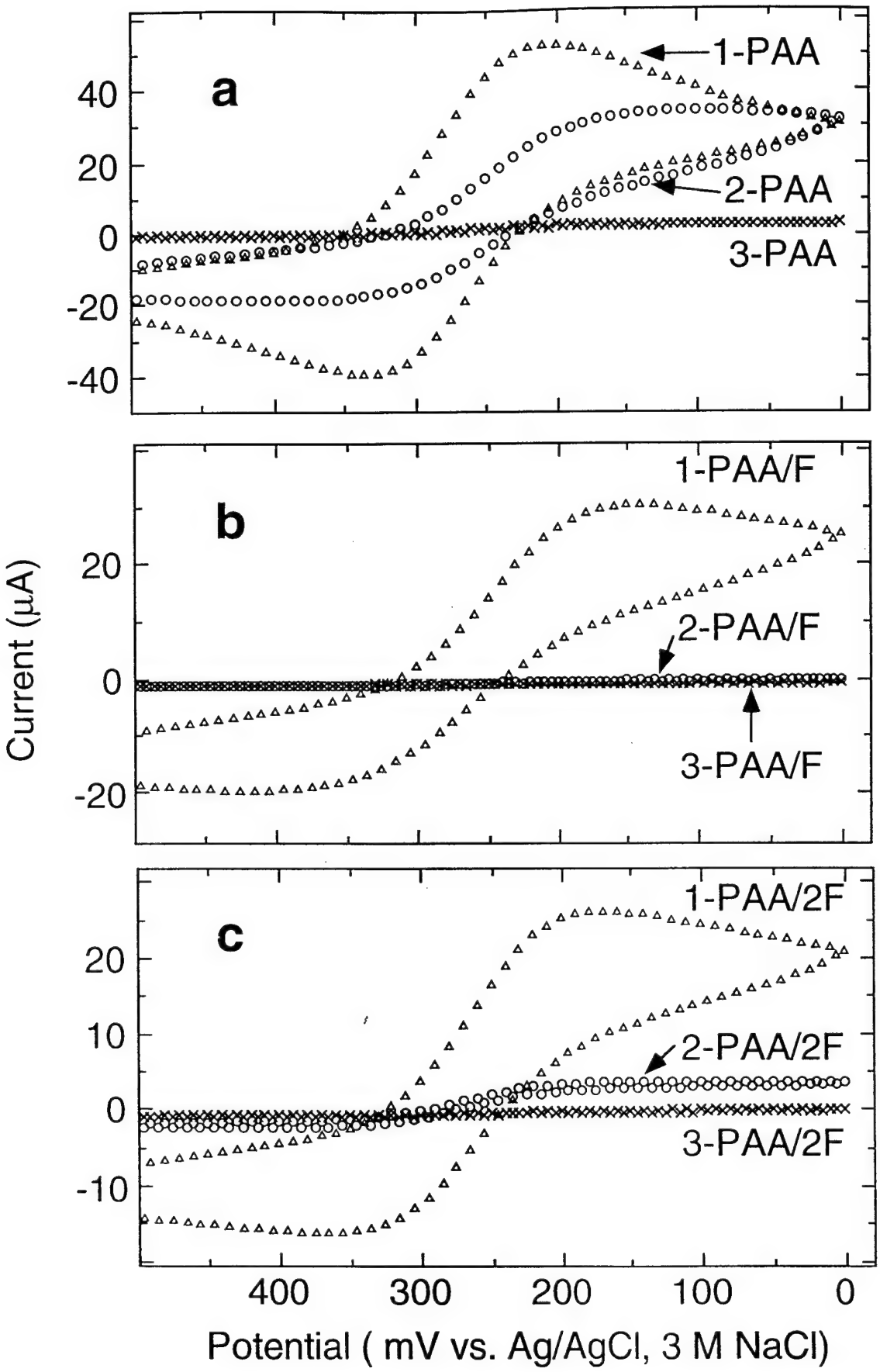

Figure 1 / Zhao et al.

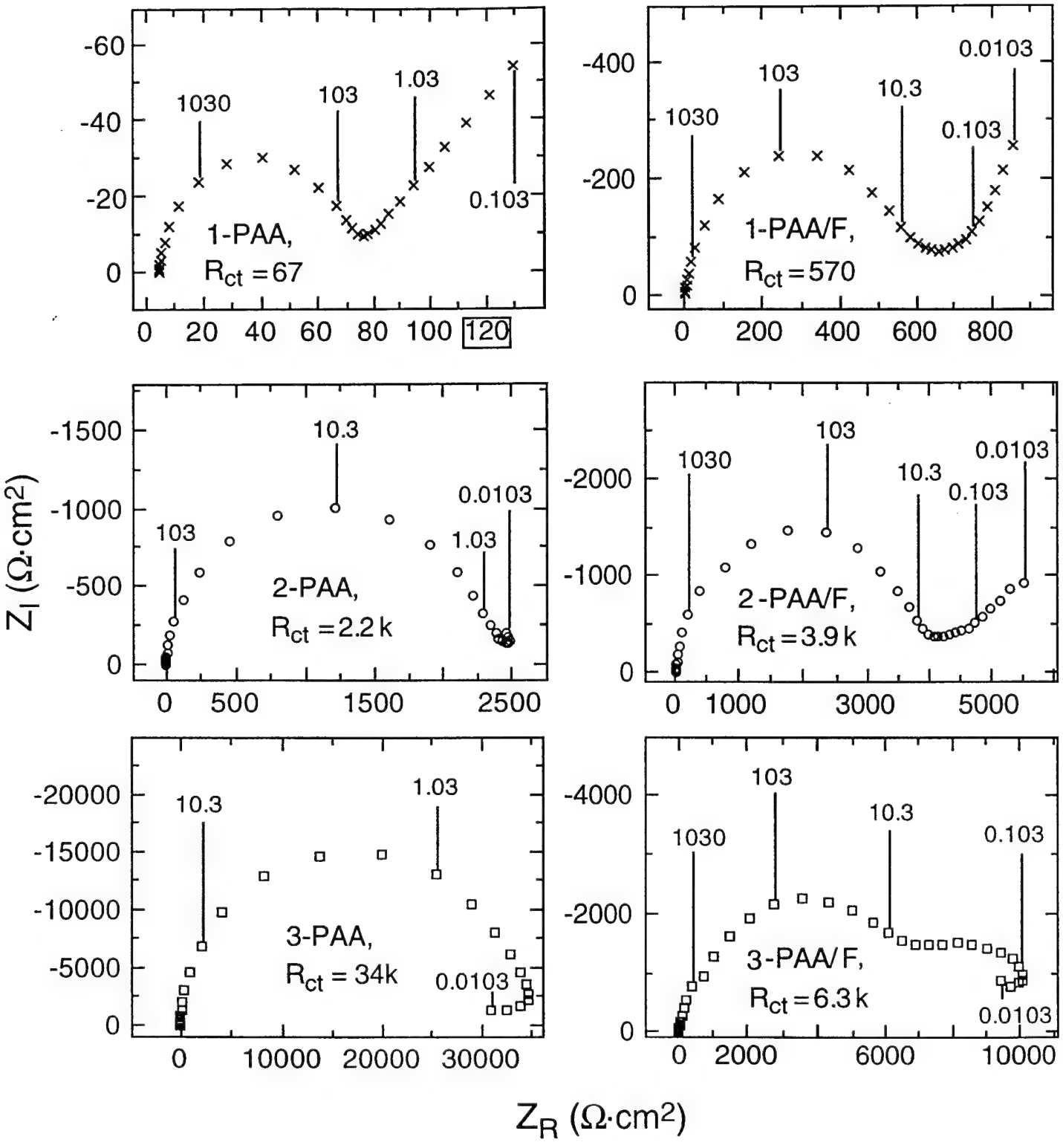

Figure 2 / Zhao et al.

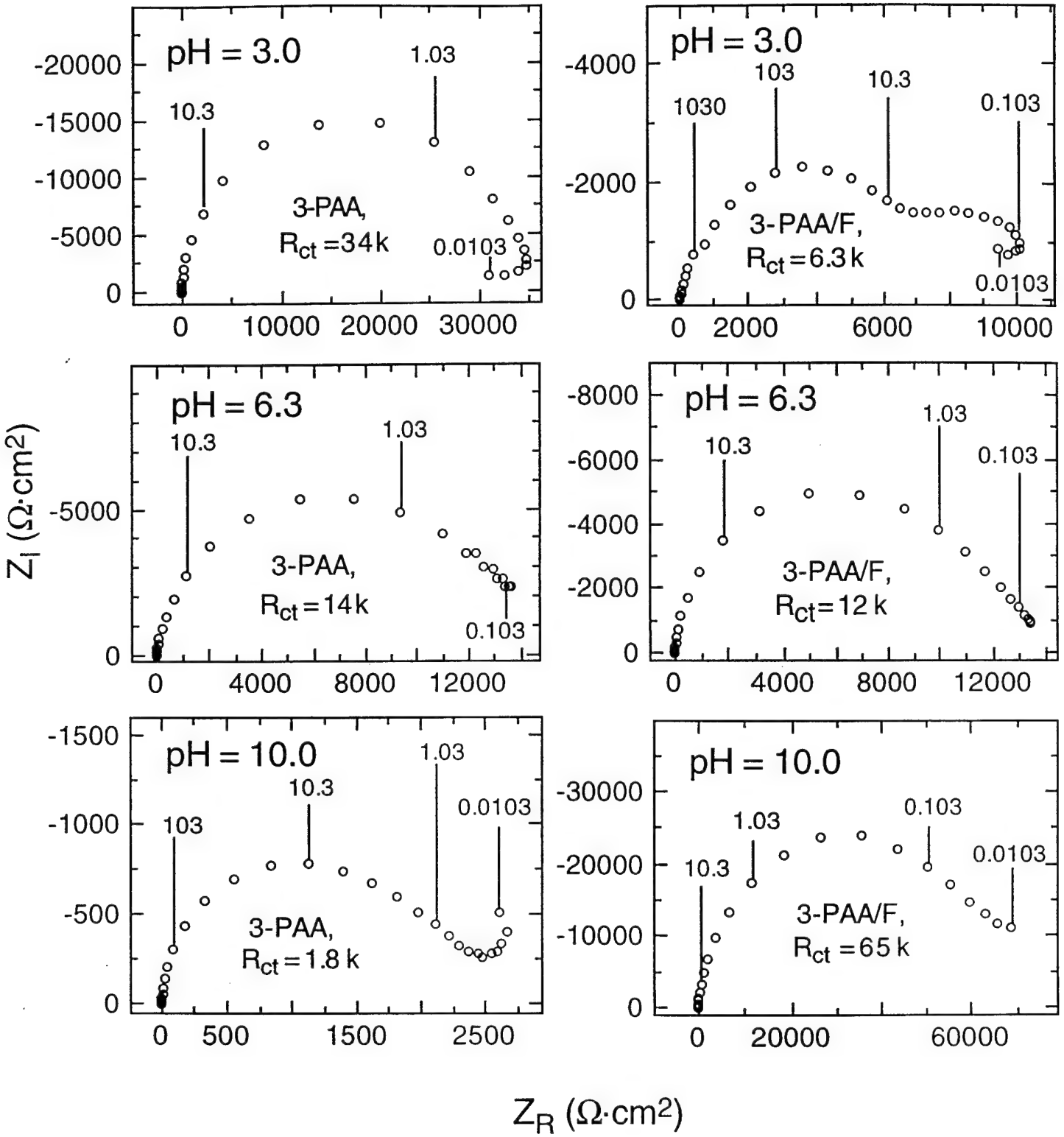

Figure 3 / Zhao et al.

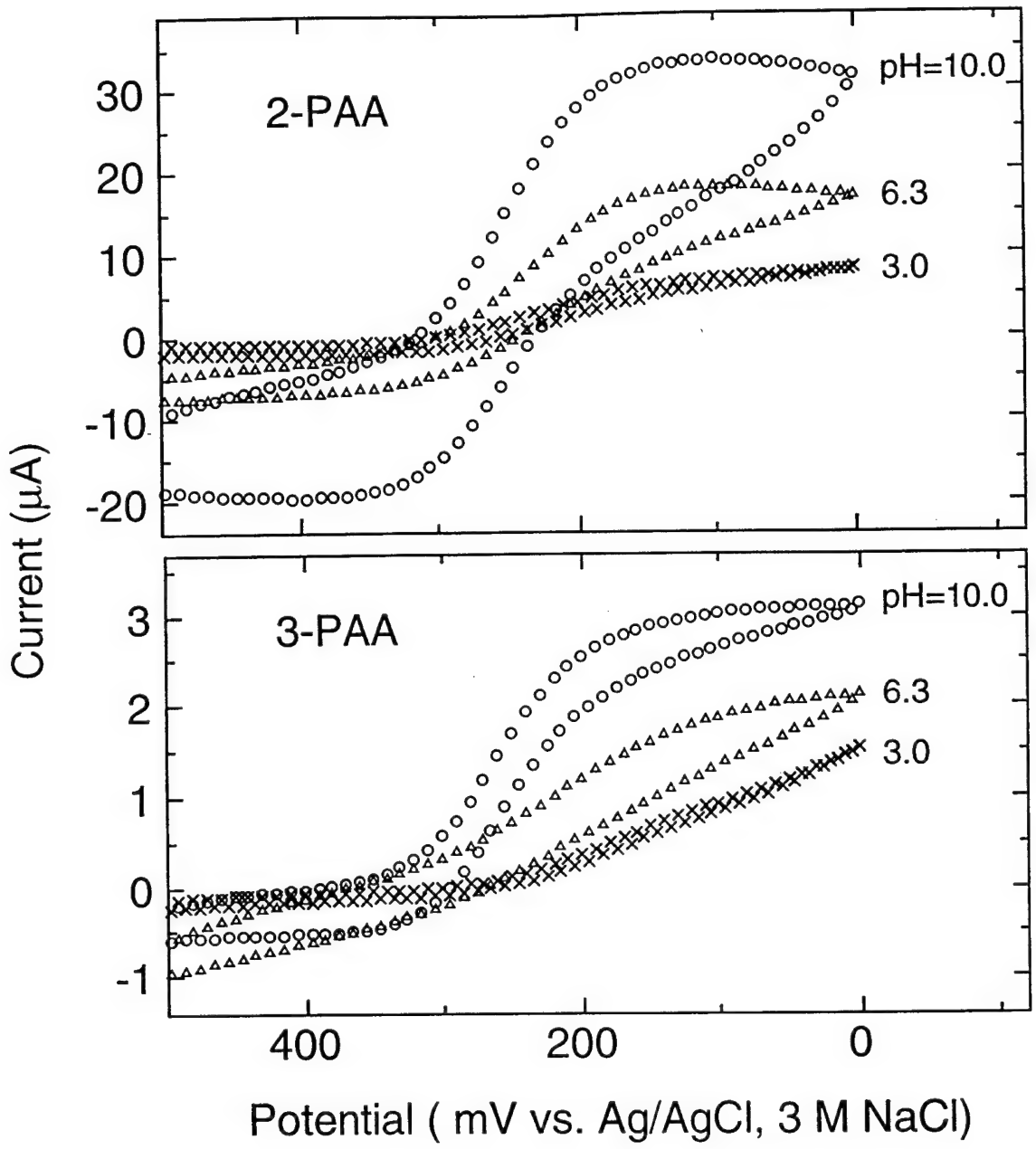

Figure 4 / Zhao et al.

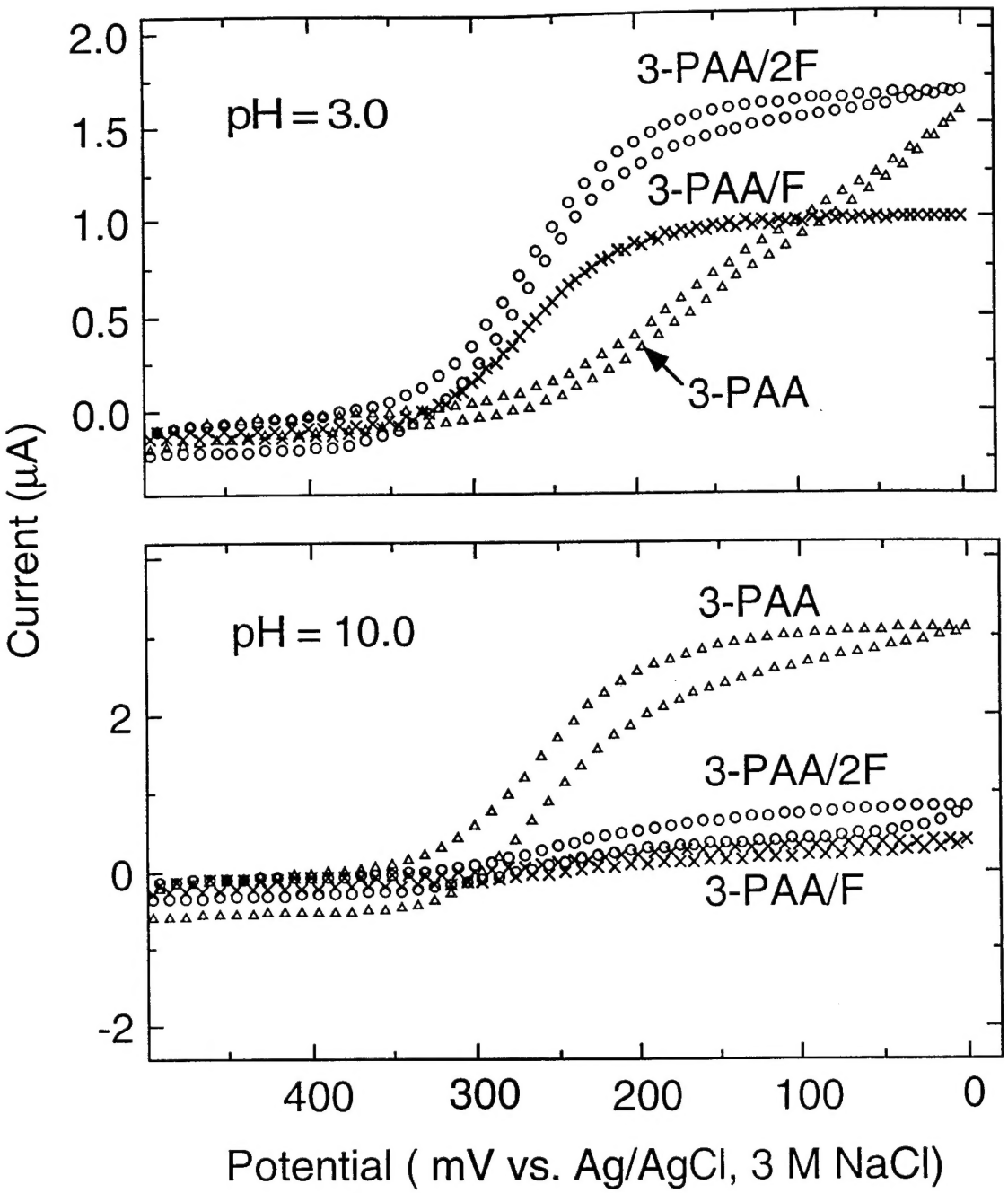

Figure 5 / Zhao et al.

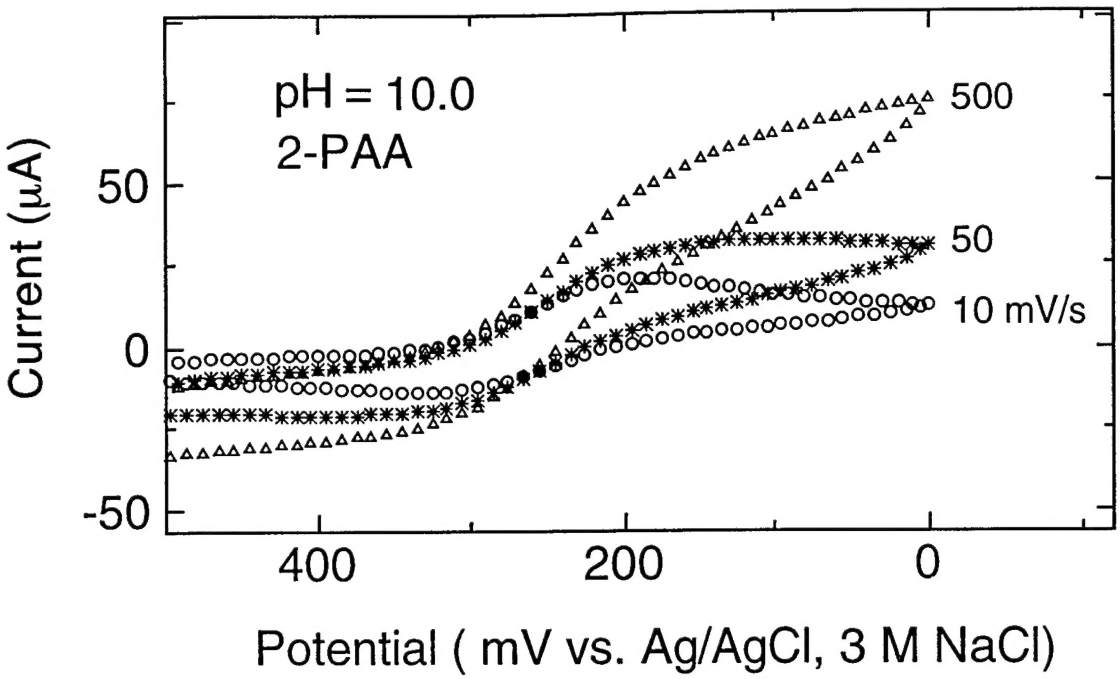

Figure 6 / Zhao et al.

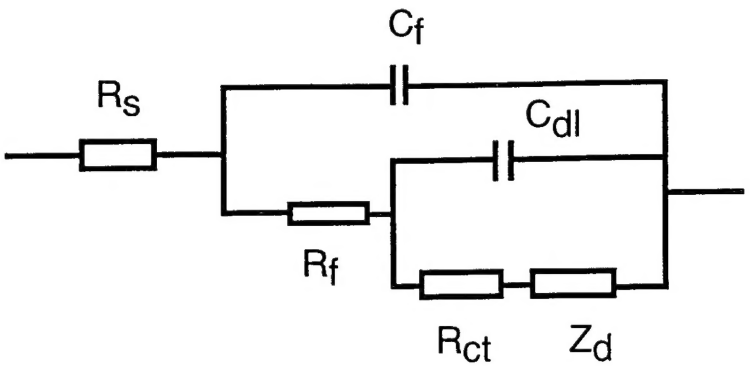

(a)

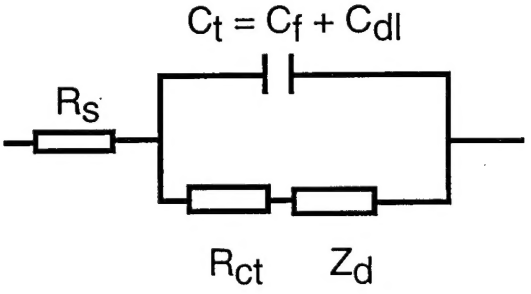

(b)

Figure 7 / Zhao et al.

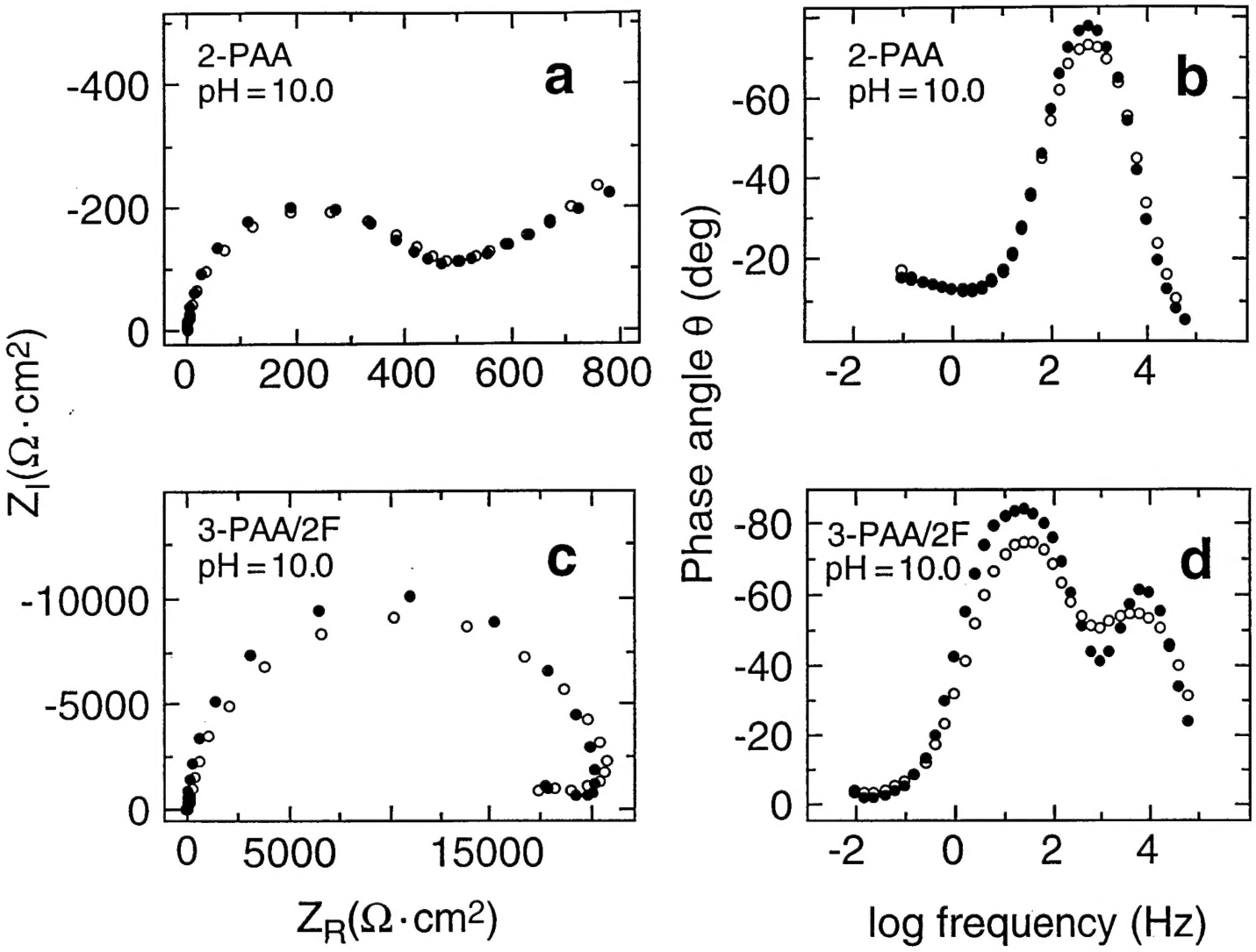

Figure 8 / Zhao et al.